NEW DATA ABOUT EVOLUTION OF THE MIDDLE JURASSIC OSTRACODS GENUS *LOPHOCYTHERE* SILVESTER-BRADLEY OF THE RUSSIAN PLATE

© 2025 Y. A. Shurupova [a,b,*]

[a] *Lomonosov Moscow State University, Moscow, Russia*

[b] *Severtsov Institute of Ecology and Evolution, Russian Academy of Sciences, Moscow, Russia*

** e-mail: shurupova.ya@yandex.ru*

Received August 23, 2024
Revised September 17, 2024
Accepted September 17, 2024

Abstract. Important for stratigraphy ostracods of the genus Lophocythere (family Progonocytheridae) from the Middle Jurassic strata of the Central European Russia (sections Mikhailovsky rudnik, boreholes № 4, № 7, Kursk region and Mikhailovcement, Ryazan region) were studied. This article provides an updated review of the evolution of this taxa, three evolutionary lineages reconstructed: L. batei Malz, 1975 → L. mosaica sp. nov., L. tuberculata sp. nov., L. karpinskyi (Mandelstam in Lyubimova, 1955); L. propinqua Malz, 1975 → L. scabra Triebel, 1951 → L. bucki Lutze, 1960; L. carinata Blaszyk, 1967 → L. interrupta Triebel, 1955 → ? → L. acrolophos Whatley, Ballent et Armitage, 2001. The evolution of the first lineage can be characterized as cladogenesis (the origin of three species from the common ancestor). The evolution of the other two lineage can be described as anagenesis (or phyletic evolution) (species successively replace each other over time). A new species Lophocythere tuberculata sp. nov. is described from the lower Callovian (Subpatruus and Koenigi ammonite zones) and upper Callovian (Athleta ammonite zone, Spinosum subzone) of the Kursk and Ryazan regions and L. mosaica sp. nov. is described from the lower Callovian (Gowerianus and Calloviense ammonite zones) of the Kursk region.

Keywords: *Ostracoda, microevolution, Middle Jurassic, Callovian, Russian Plate, cladogenesis, anagenesis*

DOI: 10.31857/S0031031X250105e9

INTRODUCTION

Ostracods of the genus Lophocythere Silvester-Bradley, 1948 appeared in the Bajocian age in the seas of Western Europe, where they existed until the beginning of the Late Jurassic epoch (Whatley, Ballent, 2004). Representatives of this genus penetrated into the Middle Russian Sea on the Russian Plate at the beginning of the Callovian age due to the marine transgression that covered Europe (Sazonova, Sazonov, 1967; Lev, Kravets, 1982). Here, lophocytheres developed throughout the entire Callovian age and disappeared at the beginning of the Oxfordian (Whatley, 1970; Pyatkova, Permyakova, 1978; Whatley et al., 2001; Tesakova, 2003, 2008, 2013; Franz et al., 2009; Wilkinson, Whatley, 2009; Tesakova et al. 2017; Shurupova, Tesakova, 2019). Representatives of this genus are used in biostratigraphy for constructing zonal ostracod scales of Europe and the Russian Plate, some of which are markers of transgressive events (Gründel, 1973; Malz, 1975; Tesakova, 2003; Nikitenko, 2009; Tesakova et al., 2017; Tesakova, Shurupova, 2018).

The first reconstructions of kinship relationships of Middle-Late Callovian representatives of lophocytheres from the Middle Russian Sea were described earlier (Shurupova, Tesakova, 2019). The objectives of this work are: to revise the evolutionary relationships of the lophocytheres of the Middle Russian Sea after a more detailed study of the ontogenesis of shell sculpture and processing of a larger sample of material covering the entire Callovian age, as well as to assess the possibility of using representatives of this genus from the Middle Russian Sea for evolutionary research and to describe two new species. The obtained data can be prospectively used for identifying phylozones, detailing and correlating zonal scales, and for paleoecological reconstructions.

MATERIAL AND METHODS

The studied ostracods of the genus Lophocythere come from several localities: Ryazan Region – Mikhailovcement section, where Middle and Late Callovian representatives were studied; Kursk Region – Mikhailovsky Mine section, boreholes No. 4 and No. 7, from which Early Callovian forms

originate. All material - samples of clays and siltstones (Mikhailovcement), washed powders (Mikhailovsky mine) and selected collections of ostracods (Mikhailovsky mine, wells No. 4 and No. 7) - was kindly provided by E.M. Tesakova, Lomonosov Moscow State University (MSU), Geological Institute of RAS (GIN RAS).

The studied sections represent alternating thinly parallel-layered clays and siltstones. The Mikhailovcement section is one of the reference sections for the Callovian-Lower Oxfordian marine deposits of the Moscow syneclise. It is a wall of the active quarry of JSC "Mikhailovcement" near the city of Mikhailov in the Ryazan region (coordinates N54.215588, E38.936135), containing rich complexes of ammonites and microfauna. Sampling, determination of the relative age of layers by ammonites, and description of the section were performed by M.A. Rogov (GIN RAS) (Tesakova et al., 2017).

The Mikhailovsky mine section is located on the territory of the Mikhailovsky GOK (mining and processing plant) quarry in Zheleznogorsk (coordinates N52.330921, E35.404383). Description of the section is presented by Tesakova et al. (2009). Well No. 4 is located in the Ponyrovsky district, between the villages of Olkhovatka and Stanovoye (coordinates N52.230369, E36.113189). Well No. 7 is in the Fatezhsky district between the hamlets of Kochetok and Malinov (coordinates N52.033136, E36.052926). Samples were collected by D.B. Gulyaev (Yaroslavl), A.V. Guzhov, Borissiak Paleontological Institute of RAS (PIN RAS) and A.V. Chereshinsky, Voronezh State University (VSU).

Collections of lophocytheres from the Mikhailovsky mine section, wells No. 4 and No. 7, are stored at the Department of Regional Geology and Earth History of the Geological Faculty of MSU (Moscow) under Nos. MSU KMA, MSU KO, MSU Kursk. From the Mikhailovcement section - at the Department of Biological Evolution of the Biological Faculty of MSU under Nos. MSU MS, MSU MS2; MSU MS2017, MSU MS2017-2.

Rock samples were washed using the standard method (boiling with soda). Ostracods from the washed powders were selected under MBS-1 or Micromed MC2 Zoom 1 CR binoculars at 10-40× magnification. The selected valves and whole shells were distributed according to age stages and gender (in adult specimens). The number of separate valves, whole shells (counted as two valves each in calculations), and fragments was counted.

The material was photographed by the author using SEM in the instrumental analytics room at PIN RAS (Cambridge CamScan-4 and TESCAN VEGA-II XMU) and in the inter-departmental laboratory of electron microscopy at the Biology Faculty of MSU (JSM-6380LA and Cambridge CamScan S-2). Each valve was photographed from outside and inside, whole shells were captured from both lateral sides, some additionally from ventral and dorsal sides. Image processing and morphometric measurements were performed using the GIMP graphic editor (V2.10.18). Only whole specimens were included in the morphometric analysis to determine age stages. Figures were made in CorelDRAW, GIMP, Excel.

To describe the shell hinge, the concept of "dental formula" is used, which is recorded as AT[G]PT, where AT – anterior tooth, [G] – groove, PT – posterior tooth (Shurupova, Tesakova, 2019). For the entomodont type hinge (for right valves), instead of letter designations, the following is indicated: the first digit – number of denticles in the anterior tooth; in square brackets – number of pits in the median groove; the last – number of elements in the posterior tooth.

The following abbreviations are used in the publication: RV – right valve of the shell; LV – left valve of the shell; Ad. – adult specimen valve; A-1–A-8 – ontogenetic stages, where A-8 is the youngest (according to Horne et al., 2002).

SYSTEMATIC PART

The systematics of suprageneric taxa follows the "Practical Guide..." (1999) with amendments in accordance with the "International Code of Zoological Nomenclature" (2004).

① ORDER PODOCOPIDA

① SUBORDER CYTHEROCOPINA

② SUPERFAMILY PROGONOCYTHEROIDEA SYLVESTER-BRADLEY, 1948

③ FAMILY NEUROCYTHERIDAE GRUENDEL, 1975

④ Genus Lophocythere Silvester-Bradley, 1948

⑤ Lophocythere tuberculata Shurupova, sp. nov.

Lophocythere scabra: Pyatkova, Permyakova, 1978, p. 145, Table 61, fig. 1, 2; Tesakova, 2013, p. 1227, Table 6. fig. 9.

Lophocythere sp. B: Tesakova, Shurupova, 2018, p. 1572, Table 10, fig. 15; Shurupova, Tesakova, 2019, p. 937, fig. 4/i.

Species name from tuberculum *Lat.* – small tubercle.

Holotype – MSU KO2-213, right valve of female; Kursk region, Ponyrovskiy district, borehole No. 4, depth 107 m (sample No. 4/123); Lower Callovian, Ostracod zone Palaeocytheridea (Malzevia) parabakirovi (ammonite zones Gowerianus and Calloviense) (Fig. 1, *a*).

Description (Figs. 1–4). Shell of medium size, moderately convex from lateral side, lenticular from dorsal side. Anterior and posterior ends flattened. Left valve overlaps right valve at anterodorsal and posterodorsal angles. Maximum length of shell is at mid-height of valve, maximum height is in anterior third at level of anterior hinge ear. Maximum thickness is in posteroventral part of shell. Dorsal margin straight, inclined towards ends of shell: smoothly joining with anterior end, with posterior end through a ledge. On left valve, dorsal margin is complicated by hinge ears with

short scalloped ridges. Ventral margin slightly convex, converging towards posterior and anterior ends, when viewed from inside, concave in anterior third. Anterior end high, rounded-arcuate, slightly oblique in upper part. Posterior end triangular, almost symmetrical, slightly more oblique from above. A narrow rim is developed at anterior end, with sparse spines located on it.

The macrosculpture includes two continuous ribs. The first is L-shaped, originating from the eye tubercle, thin along the anterior margin and thick scalloped along the ventral margin. Below is the second - ventrolateral rib, thin crest-like, running parallel to the ventral margin. These ribs extend across the entire lateral surface, not reaching the ends of the shell. Behind the L-shaped rib, there are three large spines, elliptical at the base, with scalloped tops. The first is under the eye tubercle in the anterior-median part; the second is below the first, closer to the center of the shell; the third, the largest, most rounded, is located in the center of the shell, closer to the dorsal margin.

Mesosculpture is represented by large rounded tubercles-conules with pores. On the ventral side, they line up in a row between the L-shaped and ventrolateral ribs. At the anterior end, they are parallel to the anterior margin; at the posterior end, they tend to form vertical chains. On the shells of juvenile specimens, there is a large-meshed network with thin edges between the mesosculpture tubercles. Simple (normal) and sieve-like pores are located on the mesosculpture tubercles and macrosculpture spines, as in other cytherocopins (Practical Guide..., 1989).

The eye tubercle is lens-shaped, laterally flattened, located in the anterodorsal part of the valve.

The hinge line is straight. The hinge is tripartite, of entomodont type. On right valves, it is represented by marginal teeth and a median groove (Fig. 1, *a1-g1*). The dental formula is 6[4+11~14]6. The anterior and posterior teeth consist of six elongated, upward-widening bicuspid denticles. The groove is widened in the anterior part, with four large rounded pits formed from pairs of merged pits. In the posterior part, the groove is complicated by 11-14 small separate pits.

The central muscle field has four oval adductor scars and two rounded mandibular scars. The pore-canal zone is wide, well-developed at the anterior and posterior ends of the valve (Fig. 1, *a1-c1*).

Sexual dimorphism is contoured, expressed in differences in shape and size of shells - males have larger, more elongated shells (due to which the macrosculpture elements are more massive) (Fig. 1, *c*).

Holotype dimensions in mm: length - 0.63; height - 0.32.

Ontogeny. *Shell hinge* . On right valves at stages A-4 - A-2, the anterior tooth consists of five, the posterior of six denticles. The median groove is finely and uniformly notched, consisting of approximately 20 rounded pits. At stage A-1, the anterior and posterior teeth have six denticles each, in the anterior half of the groove four large pits from merged pairs of smaller pits are clearly visible. In adult specimens, the structure remains unchanged, the groove elements increase in size (Fig. 1, *a1-d1*; 2).

Shell sculpture. Macrosculpture is well distinguishable on shells of all ages. In early stages, it is represented by thin L-shaped and ventrolateral ribs with scalloped tops; spines are rounded. With age, macrosculpture elements increase in size, ribs become thicker, spines more crest-like. Mesosculpture in juvenile specimens is represented by conules, with a coarse-meshed network with thin edges between them. With age, the network edges become smoother. In adult specimens, conules increase in size and arrange in rows.

The eye tubercle in early ontogenetic stages is weakly expressed, hidden under a large downward-descending L-shaped rib. With age, the size ratio between the eye tubercle and rib changes: the tubercle becomes larger, while the rib on it becomes smaller.

Variability. It is slightly expressed in variations of L-shaped and ventrolateral rib thickness, sizes of spines and conules, and in the degree of conule chain fusion into rows at the posterior end of the shell. In Lower Callovian deposits, four specimens were found with the largest conules of mesosculpture merging into vertical ribs (Fig. 3). Early Callovian adult specimens show various dental formulas in the shell hinge (some examples see: Fig. 4). In females: 6[3:20]6; 6[4:14]6; 6[4:15]6; 6[4:20]6; 6[6:11]6; 6[6:10:2]6; 6[8:4]6; 6[11:0]6; 6[4:14]6. In males: 6[4:>20]6; 6[5:14]6;

6[6:10:2]6; 6[9:4]6; 6[13:0]6; 6[11:0]6 (with elongated pits in the groove instead of rounded paired ones). An aberrant form with dental formula 5[4:14]5 was found (Fig. 4, *d*).

Age-related changes are manifested in size (Fig. 5) and shell shape: the younger the age stage, the more triangular the shell outline becomes. Sculpture of juvenile specimens is more gracile.

C o m p a r i s o n . L. tuberculata sp. nov. differs from L. mosaica sp. nov., L. scabra Triebel, 1951, L. karpinskyi (Mandelstam in Lyubimova, 1955) and L. bucki Lutze, 1960 in shell sculpture, which is characterized by a continuous L-shaped rib on the ventral side. In L. scabra it is also continuous but thinner; breaks into separate spines in L. mosaica sp. nov. and L. bucki in the posterior part, in L. karpinskyi entirely. In L. tuberculata sp. nov. the macrosculpture spines and mesosculpture conules are large, with rounded tops; in L. mosaica sp. nov. the spines are smaller, less rounded. In L. scabra and L. bucki they are also smaller, merging into thin vertical ribs. In L. karpinskyi, the conules in the anterior part of the shell are similar in size but more rounded at the base, in the posterior part they are smaller. In L. tuberculata sp. nov. the mesosculpture mesh develops from large-celled, as in L. mosaica sp. nov. and L. karpinskyi; differs from the fine-celled mesh of L. scabra and L. bucki. In the new species (in typical representative) the dental formula of the shell hinge 6[4+11~14]6 differs in the structure of the groove : in L. karpinskyi 6[5+11]6; in L. bucki 6[6+14]6; in L. scabra 6[4+12~14]6; in L. mosaica sp. nov. 6[4+14].

D i s t r i b u t i o n . Callovian stage; Kursk and Ryazan regions [ostracod zone Palaeocytheridea (Malzevia) parabakirovi (ammonite zones Gowerianus and Calloviense), ammonite zones Subpatruus and Koenigi to the boundary of Lamberti - Athleta zones, subzone Spinosum], Dnepropetrovsk-Donetsk depression, Sumy region of Ukraine.

M a t e r i a l . More than 200 specimens (separate valves, complete shells of adult and juvenile specimens) of good and satisfactory preservation from the Lower Callovian deposits of the Mikhailovsky mine section, boreholes No. 4 and No. 7 (Kursk region) and one specimen of good preservation from the Upper Callovian deposits of the Mikhailovcement section (Ryazan region).

Lophocythere mosaica Shurupova, sp. nov.

Species name mosaica *Latin* - mosaic.

Holotype - MSU KO2-161, right valve of female; Kursk region, Ponyrovsky district, borehole No. 4, depth 101.1 m (sample No. 4\116); Lower Callovian, ostracod zone Palaeocytheridea (Malzevia) parabakirovi (ammonite zones Gowerianus and Calloviense) (Fig. 6, *a*).

Description (Fig. 6). The shell is medium-sized, moderately convex from the lateral side, lens-shaped from the dorsal side. The anterior and posterior ends are flattened. The greatest length of the shell occurs at mid-height of the valve, the greatest height is in the anterior third at the level of the anterior hinge ear, the greatest thickness is in the posterior-ventral part of the shell. The dorsal margin is straight, sloping towards the ends of the shell, smoothly conjugating with the anterior end and through a ledge with the posterior end. On the left valve, the dorsal margin is complicated by hinge ears with large scalloped ridges. The ventral margin is slightly convex, converging towards the posterior and anterior ends, when viewed from inside, it is concave in the anterior third. The anterior end is high, rounded-arcuate, slightly oblique in the upper part. The posterior end is triangular, practically symmetrical, slightly more oblique from above. At the anterior end, there is a narrow rim with sparse tubercles.

The macrosculpture includes two ribs. The first is an intermittent L-shaped rib, originating from the eye tubercle. It extends along the anterior end and ventral margin, continuous in the anterior half of the shell, breaking into separate large spines in the middle and posterior parts. Below is the second - ventrolateral rib, thin, crest-like; extending across the entire lateral surface, not reaching the ends of the shell. Behind the L-shaped rib along the anterior end of the shell, there are two short intermittent ribs, ellipsoid at the base, with flattened scalloped tops. The first is under the eye tubercle in the anterior-median part; the second is lower, closer to the central part of the shell. In the center of the shell near the dorsal margin is the largest spine, flattened on the sides, with a scalloped top.

The mesosculpture is represented by a thin intermittent rib on the ventral side between the macrosculpture elements and small tubercles-conules, arranging themselves in vertical chains at the ends of the shell. Between the chains, there is a weakly expressed large-meshed network with thin edges. In the center of the shell, the valve surface is smooth. Simple (normal) and sieve-like pores are located on the mesosculpture tubercles, spines, and macrosculpture ribs.

The eye tubercle is lens-shaped, flattened on the sides, located in the anterior-dorsal part of the valve.

The hinge line is straight. The hinge is three-membered, of entomodont type. On the right valves, it is represented by marginal teeth and a median groove (Fig. 6, *a1-d1*). The anterior and posterior teeth consist of six elongated, upward-widening denticles with rounded tops. The dental formula is 6[4+14]6. The groove is widened in the anterior part, with four large rounded pits, each formed by a pair of merged pits. In the posterior part, the groove is complicated by 14 small separate rounded pits.

The central muscle field has four oval adductor scars and two rounded mandibular scars. The pore-canal zone is wide, well-developed at the anterior and posterior ends of the valve (Fig. 6, *a1-c1*).

Holotype dimensions in mm: length - 0.62; height - 0.33.

Ontogeny. The material does not allow for a detailed description of ontogeny, as not all growth stages were found - besides adult specimens, only juvenile stages A-2 - A-1 are known.

Shell hinge. At stage A-2, the anterior tooth consists of five denticles, the posterior of six denticles, the median groove is finely notched with rounded pits. For stage A-1, the hinge structure is unknown.

Shell sculpture. At stages A-2 - A-1, the macrosculpture is represented by fine ribs: L-shaped, which breaks into separate spines along the ventral margin, and ventrolateral. Behind the L-shaped rib are three large spines on an elliptical base, with a festooned apex. The mesosculpture at these stages is represented by a coarse-meshed network with thick edges and large sparse conulae at the

nodes. In adult specimens, a weakly expressed network remains on the anterior and posterior ends, the macrosculpture spines merge into short vertical ribs, their base becomes more elongated. The L-shaped rib in the anteroventral part becomes more monolithic.

The eye tubercle at stages A-2 and A-1 is weakly expressed, hidden under a large downward-extending L-shaped rib. With age, the size ratio of the eye tubercle and rib changes: the tubercle becomes larger, the rib on it becomes smaller.

Variability. Variability is expressed in minor variations in size and degree of fusion of macrosculpture spines, degree of fusion of mesosculpture tubercles into chains, and height of projections above the hinge ears on the left valves.

Age variability is expressed in the size and shape of the shell: the younger the age stage, the more triangular the shell outline becomes. The sculpture in juvenile specimens is more gracile.

Comparison L. mosaica sp. nov. differs from L. tuberculata sp. nov., L. scabra, L. karpinskyi, and L. bucki in its macrosculpture - the spines are larger, on an elliptical base, and merge into short vertical ribs. The L-shaped rib discontinuous along the ventral margin in the new species is thicker than in L. bucki. It differs from the continuous L-shaped rib of L. scabra and the completely separated into individual spines rib of L. karpinskyi. In L. mosaica sp. nov., the conules and mesosculpture ribs are larger than in L. bucki. The large-meshed network of mesosculpture in ontogenesis of L. mosaica sp. nov. is more pronounced, with higher walls than in L. karpinskyi. In L. scabra and L. bucki species, the mesosculpture forms from a finer-meshed network. In L. mosaica sp. nov., the structure of the median groove in the shell hinge differs: dental formula 6[4+14]6, while in L. karpinskyi it is 6[5+11]6, and in L. scabra 6[4+12~14]6. In the hinge teeth, the denticles of L. mosaica sp. nov. have rounded apex, unlike the bifid ones in L. karpinskyi, L. scabra, and L. bucki. Comparison with L. tuberculata sp. nov. is presented in the description of that species.

Distribution Lower Callovian substage [ostracod zone Palaeocytheridea (Malzevia) parabakirovi (ammonite zones Gowerianus and Calloviense)], Kursk region.

Material 22 specimens (separate valves of adult and juvenile individuals) of varying preservation from Lower Callovian deposits of the Mikhailovsky quarry section, boreholes No. 4 and No. 7 (Kursk region).

DISCUSSION

Lophocytheres entered the Middle Russian Sea during the Early Callovian with transgression from Western Europe. Here, L. mosaica sp. nov., L. scabra, and L. interrupta are known from Lower Callovian deposits. L. karpinskyi occurs from the beginning of the Callovian to the beginning of the Oxfordian. The history of L. tuberculata sp. nov. spans the entire Callovian age.

The appearance of L. bucki and L. Acrolophos in the Late Callovian is apparently associated with another transgressive event from Western Europe in the Athleta phase; these species are markers of transgressive events (Tesakova et al. 2017; Tesakova, Shurupova, 2018).

The studied Lophocythere can be divided into three evolutionary branches (Fig. 7, *a*). The first one (Fig. 7, *a1*) descended from the ancestral species L. batei Malz, 1975, known from the Middle and Upper Bathonian deposits of England (Malz, 1975; Whatley, Ballent, 2004). This branch includes L. tuberculata sp. nov. (Fig. 1), L. mosaica sp. nov. (Fig. 6), and L. karpinskyi (Table VI, fig. 7-9). In L. batei, the macrosculpture consists of continuous L-shaped and ventral ribs and large spines in the central part of the valve. Other conuli on the shell surface are arranged in vertical chains. The L-shaped rib on the ventral side in L. mosaica sp. nov. is interrupted in the posterior part; in L. tuberculata sp. nov. it is continuous; in L. karpinskyi it consists of large spines. In their ontogenesis, the mesosculpture develops from a coarse-meshed network with rare conuli at the intersection of edges. This feature appears on the shells of juvenile specimens in L. batei ancestors (Malz, 1975) and persists in descendants. In all adult specimens of L. tuberculata sp. nov. and L. karpinskyi, the mesosculpture between spines and conuli smooths out, while in L. mosaica sp. nov. it remains weakly expressed at the anterior and posterior ends.

The second evolutionary branch (Fig. 7, *a2*) originates from L. propinqua Malz, 1975, known from the Upper Bathonian deposits of England and France (Malz, 1975; Whatley, Ballent, 2004). From it, in the Early Callovian age, L. scabra evolved (Table VI, fig. 10-12), which gave rise to L. bucki (Table VI, fig. 13-15) in the Late Callovian. The sculpture of representatives of this branch consists of thin ridge-like ribs: L-shaped, ventrolateral, and interrupted vertical ones. In the evolution of Callovian species, the ribs in the shell sculpture broke down into separate spines. L. scabra retains continuous L-shaped and ventrolateral ribs, and interrupted vertical ones. In the later L. bucki, the ventrolateral and vertical ribs remain, while the L-shaped rib breaks down into spines in the posterior part. The mesosculpture of ostracods in this evolutionary branch develops from a fine-meshed network (the ontogenesis of L. propinqua is unknown). In L. scabra, at early juvenile stages, the mesosculpture network has rare small conuli (Table VI, fig. 12). In L. bucki, the mesosculpture network has conuli and very small tubercles (Table VI, fig. 14, 15).

In L. batei, individual spines are larger, with a rounded base, which makes the appearance of representatives of this group more "spiny". In L. propinqua, the sculpture consists of thin interrupted ribs, making the appearance of representatives of this evolutionary branch more "ribbed".

The third evolutionary branch of Lophocythere (Fig. 7, *a3*) most likely originates from L. carinata Blaszyk, 1967, known from Bathonian deposits of Poland and Germany (Blaszyk, 1967; Malz, 1975; Whatley, Ballent, 2004). In the Early Callovian, L. interrupta (Table VI, fig. 1-3) evolved from it, which later gave rise to L. acrolophos (Table. VI, fig. 4-6) in the Late Callovian (Shurupova, Tesakova, 2019; Shurupova, 2023). The macrosculpture of representatives of this group differs significantly from that of the evolutionary branches discussed above. It is represented by solid ribs: L-shaped, ventrolateral, and three vertical - curved, short, not reaching the ventral part of the L-shaped rib. Conulae and spines, characteristic of other studied Lophocythere, are absent.

In the ancestral species L. carinata, a prominent coarse-meshed network of mesosculpture is clearly expressed between the macrosculpture ribs across the entire valve surface. This feature can be

traced in the descendant L. interrupta from the earliest juvenile stages. In the later L. acrolophos, the network is very weakly expressed at all age stages. Since the mesosculpture of these species differs from the earliest stages, there might have existed an unknown transitional form during the Middle Callovian (Shurupova, Tesakova, 2019; Shurupova, 2023), this is marked in Fig. 7, *a3* with a question mark.

In R. Whatley's publication (Whatley, 1970), reconstructions of relationships are proposed for some of the studied Lophocythere. The species L. scabra is indicated as ancestral to L. interrupta. Both species are known from the Early Callovian, but their sculpture differs significantly. L. interrupta has solid macrosculpture ribs, a prominent coarse-meshed mesosculpture network without conulae at all age stages (Pl. VI, fig. 1-3), while L. scabra has thinner and interrupted vertical ribs, and the mesosculpture network edges are weakly expressed and have conulae (Table VI, fig. 10-12).

In L. Sheppard's dissertation (Sheppard, 1981), different evolutionary relationships are reconstructed (Fig. 7, *b*): the species L. ostreata (Jones et Sherborn, 1888), known from Bathonian deposits of England (Malz, 1975) and France (Oertli, 1963), is considered ancestral to L. carinata and L. batei. L. propinqua originates from the latter, which is the ancestor of L. scabra and L. karpinskyi. It is noted that the evolution of shell sculpture in these species proceeded through the reduction of mesosculpture grid and development of large macrosculpture elements.

However, the shell sculpture in L. ostreata differs significantly from that of L. batei and other studied lophocytherids. The macrosculpture of L. ostreata is more gracile, with fine ribs, and the mesosculpture is represented by a large-meshed grid, without vertical ribs and conulae. Additionally, the shell shape of L. ostreata is more rectangular.

In the article by Ya.A. Shurupova and E.M. Tesakova (Shurupova, Tesakova, 2019), different evolutionary branches are reconstructed for some of the studied lophocytheres (Fig. 7, *c*). The first one - L. karpinskyi → L. bucki (L. sp. A in the cited work) is distinguished based on similarities in the shell hinge and L-shaped rib in the ventral part (Fig. 7, *c1*). However, studying a larger sample of

ostracods of this genus revealed that L. karpinskyi has more massive and rounded spine macrosculpture at the base, and its sculpture has more similarities with L. batei. While L. bucki's mesosculpture in ontogenesis is represented by a fine-meshed network (unlike the coarse-meshed in L. karpinskyi), the macrosculpture ribs are thin (like in L. scabra). The second proposed evolutionary branch (Shurupova, Tesakova, 2019): L. propinqua → L. scabra → ? → L. tuberculata sp. nov. (L. sp. B in the cited work) (Fig. 7, *c2*). The question mark (here and in Fig. 7) indicates that there might have been an unknown transitional form between these species. Similar elements are noted: an unsegmented L-shaped rib in the ventral part and vertical ribs made of conule chains. The sculpture in L. propinqua and L. scabra has a similar appearance - thin ribs made of spines and conules. However, L. tuberculata sp. nov. sculpture differs from these species by having more massive ribs and spines. The reconstruction of the third evolutionary branch (also described in: Shurupova, 2023) - L. interrupta → ? → L. acrolophos - remains unchanged in this work (Fig. 7, *c3*). And L. carinata is proposed as the most suitable ancestral species based on the similarity of shell sculpture: continuous macrosculpture ribs and coarse-meshed mesosculpture network.

According to the latest studied data, the evolution of the Lophocythere branch, originating from L. batei (Fig. 7, *a1*), can be characterized as cladogenesis: three daughter species descended from one ancestral species. The evolution of lophocyteres descended from L. propinqua (Fig. 7, *a2)* and from L. carinata (Fig. 7, *a3*) can be described as phyletic evolution, or anagenesis: species successively replaced each other over time, without the emergence of sister groups. According to Sheppard (1981), the evolution of some Callovian lophocyteres can be described as cladogenesis (Fig. 7, *b*). According to Shurupova and Tesakova (2019), one can distinguish a variety of cladogenesis - "lateral cladogenesis" ("budding cladogenesis" in: Foote, 1996): when the ancestral species does not disappear after a lateral evolutionary branch of descendants separated from it (Fig. 7, *c1*). For the other two branches (Fig. 7, c*2, c3*) anagenesis can be noted.

Evolutionary terminology is adopted according to works: Simpson, 1948; Grant, 1991; Foote, 1996; Futuyma, Kirkpatrick, 2017.

CONCLUSION

As a result of studying new material and detailed analysis of shell sculpture ontogenesis, refined reconstructions of phylogenetic relationships for Middle Jurassic ostracods Lophocythere are proposed. They can be divided into three evolutionary branches (Fig. 7, *a*): L. batei → L. mosaica sp. nov., L. tuberculata sp. nov., L. karpinskyi (sculpture characterized by large spines); L. propinqua → L. scabra → L. bucki (interrupted ribs are pronounced in sculpture); L. carinata → L. interrupta → ? → L. acrolophos (sculpture represented by continuous ribs and large mesh).

It is shown that lophocyteres from the Middle Russian Sea, due to their long history in this paleobasin, diversity of species within the genus, and pronounced shell sculpture, are a convenient and promising model object for evolutionary research and study of long-term evolutionary processes.

ACKNOWLEDGMENTS

The author expresses deepest gratitude to reviewer L.M. Melnikova (PIN RAS) for valuable advice on improving the article and discussing the text. The author also expresses appreciation to A.Yu. Zhuravlev (MSU, PIN RAS), E.M. Tesakova (MSU, GIN RAS), and S.N. Lysenkov (MSU) for comprehensive help and support.

FUNDING

This work was funded by a grant from the Russian Science Foundation (project No. 22-14-00258). No additional grants were received for conducting or supervising this specific research.

CONFLICT OF INTERESTS

The author of this work declares no conflict of interest

REFERENCES

1. *Grant V.* The Evolutionary Process. Moscow: Mir, 1991. 488 p.

2. *Lev O.M., Kravets V.S.* Jurassic ostracods of the Timan-Pechora region and their stratigraphic significance // Stratigraphy of Triassic and Jurassic deposits of oil and gas basins of the USSR. Leningrad, 1982. P. 65-78.
3. International Code of Zoological Nomenclature. 4th ed. Moscow: KMK Scientific Press, 2004. 223 p.
4. *Nikitenko B.L.* Stratigraphy, paleobiogeography and biofacies of the Jurassic of Siberia based on microfauna (foraminifera and ostracods). Novosibirsk: Parallel, 2009. 680 p.
5. Practical Guide to Microfauna of the USSR. Vol. 3. Cenozoic Ostracods / Ed. B.S. Sokolov. Leningrad: Nedra, 1989. 233 p.
6. Practical Guide to Microfauna. Vol. 7. Mesozoic Ostracods / Ed. B.S. Sokolov. St. Petersburg: VSEGEI, 1999. 244 p.
7. *Pyatkova D.M.*, *Permyakova M.N.* Foraminifera and ostracods of the Jurassic of Ukraine. Kiev: Naukova Dumka, 1978. 289 p.
8. *Sazonova I.G., Sazonov N.T.* Paleogeography of the Russian Platform during the Jurassic and Cretaceous periods. Leningrad: Nedra, 1967. 260 p. (Proceedings of the Research Institute of Geological Exploration for Oil. Issue 62).
9. *Simpson G.G.* Tempo and Mode in Evolution. Moscow: Foreign Literature Publishing House, 1948. 360 p.
10. *Tesakova E.M., Strezh A.S., Gulyaev D.B.* New ostracods from the Lower Callovian of Kursk Region // Paleontological Journal. 2009. No. 3. P. 25-36.
11. *Tesakova E.M., Shurupova Y.A., Ustinova M.A.* Stratigraphy of the Callovian and Lower Oxfordian of the Mikhailovcement section (Ryazan Region) based on microfauna and nannoplankton // Proceedings of the Geological Institute RAS. 2017. Vol. 615. P. 264-300.
12. *Shurupova Y.A.* Heterochrony and sexual dimorphism in Middle Jurassic Lophocythere Sylvester-Bradley, 1948 (Ostracoda, Crustacea) of the Russian Plate // Jurassic System of

Russia: Problems of Stratigraphy and Paleogeography. Proceedings of IX All-Russian Meeting: Syktyvkar, September 9-16, 2023 / Eds. M.A. Rogov, E.V. Shchepetova, A.P. Ippolitov, E.M. Tesakova. Syktyvkar: IG Komi SC UB RAS, 2023. P. 172-174.

13. *Blaszyk J.* Middle Jurassic ostracods of the Czestochowa region (Poland) // Acta Palaeontol. Pol. 1967. V. 12. № 1. P. 1–75.
14. *Foote M.* On the probability of ancestors in the fossil record // Paleobiology. 1996. V. 22. № 2. P. 141–151.
15. *Franz M., Tesakova E.M., Beher E.* Documentation and revision of the index ostracods from the Lower and Middle Jurassic in SW Germany according to Buck (1954) // Palaeodiversity. 2009. V. 2. P. 119–167.
16. *Futuyma J.D., Kirkpatrick M.* Evolution (4th Ed.). Sinauer, Sunderland, MA: Sinauer Associates, 2017. 599 p.
17. *Gründel J* . Zur Fassung der Gattung Lophocythere (Ostracoda, Crustacea) // Z. Geol. Wiss. Berlin. 1973. Bd. 1. № 5. S. 581–585.
18. *Horne D.J., Cohen A., Martens K.* Taxonomy, morphology and biology of Quaternary and living Ostracoda // The Ostracoda: Applications in Quaternary Research. 2002. P. 5–36 (Geophys. Monogr. Ser., V. 131).
19. *Malz H.* Ostracoden-Studien im Dogger, 8: Die Arten der Gattung Lophocythere, ihre stratigraphische und regionale Verbreitung // Senckenb. Lethaea. 1975. V. 56. № 2/3. S. 123–145.
20. *Oertli H.J.* Ostracoden als Salzgehalts-Indikatoren im obern Bathonien des Boulonnais // Eclog. Geol. Helv. 1975. V. 50. № 2. P. 279–283.
21. *Sheppard L.M.* Middle Jurassic Ostracoda from Southern England and Northern France. Thesis Ph.D. Univ. of London, 1981. 214 p.

22. *Shurupova Ya.A., Tesakova E.M.* Species interrelatedness in the genus Lophocythere Silvester-Bradley, 1948 (Ostracoda) in the Late Callovian of the Russian Plate // Paleontol. J. 2019. V. 53. № 9. P. 54–59.
23. *Tesakova E.M.* Callovian and Oxfordian ostracodes from the Central region of the Russian Plate // Paleontol. J. 2003. V. 37. Suppl. № 2. P. 107–227.
24. *Tesakova E.* Late Callovian and Early Oxfordian ostracods from the Dubki section (Saratov area, Russia): implications for stratigraphy, paleoecology, eustatic cycles and palaeobiogeography // N. Jb. Geol. Paläontol. Abh. 2008. V. 249. № 1. P. 25–45.
25. *Tesakova E.M.* Ostracode-based reconstruction of paleodepths in the Early Callovian of the Kursk region, Central Russia // Paleontol. J. 2013. V. 47. № 10. P. 1214–1229.
26. *Tesakova E.M., Shurupova Ya.A* . Ostracod analysis of the Callovian and Lower Oxfordian deposits of the Mikhailovtsement section (Ryazan region): methods and results // Paleontol. J. 2018. V. 52. № 13. P. 1561–1582.
27. *Whatley R.C.* Scottish Callovian and Oxfordian Ostracoda // Bull. Brit. Mus. (Natur. Hist.) Geol. 1970. V. 19. № 6. P. 299–358.
28. *Whatley R.C., Ballent S., Armitage J.* Callovian Ostracoda from the Oxford Clay of southern England // Rev. Españ. Micropaleontol. 2001. V. 33. № 2. P. 135–162.
29. *Whatley R.C.*, *Ballent S.* A review of the Mesozoic ostracod genus Lophocythere and its close allies // Palaeontology. 2004. V. 47. Pt 1. P. 81–108.
30. *Wilkinson I.P., Whatley R.C.* Upper Jurassic (Callovian–Portlandian) // Ostracods in British Stratigraphy / Eds. J.E. Whittaker, M.B. Hart. Geol. Soc. London, 2009. P. 241–287 (TMS Spec. Publ. № 3).

Figure captions

Fig. 1. Lophocythere tuberculata sp. nov., SEM, *a* - *d* - external view, *a1* - *g1* - internal view: *a* - holotype KO2-213, Ad., RV, female, sample No. 4\123; *b* - specimen KO2-176, Ad., LV, female, sample No. 4\121; *c* - specimen KO2-171, Ad., RV, male, sample No. 4\121; *d* - specimen KO1-91, A-3, RV, sample No. 4\124; *e* - specimen KO2-31, Ad., female, dorsal view, sample No. 4\125 ; Kursk region, borehole No. 4; Lower Callovian, ammonite zones Gowerianus and Calloviense. Scale bar 100 μm.

Fig. 2. Development scheme of the hinge in Lophocythere tuberculata sp. nov. during ontogeny for RV. Black indicates the marginal hinge elements, white - median groove.

Fig. 3. Variability of shell sculpture in Early Callovian Lophocythere tuberculata sp. nov., SEM, external view: *a* - specimen KMA-124, Ad., LV, female, sample No. KMA-8; *b* - specimen KMA(1-14)-5, Ad., LV, female, sample No. KMA-12; *c* - specimen KMA2-86, Ad., RV, male, sample No. KMA-8; *d* - specimen KMA2-87, RV, male, sample No. KMA-8; Kursk region, Mikhailovsky quarry section. Scale bar 100 μm.

Fig. 4. Variation in the hinge structure of Early Callovian Lophocythere tuberculata sp. nov., SEM, Ad., dorsal margin with different dental formulae: *a* – 6[6:10:2]6, specimen Kursk-22, LV, female, sample No. 14.8$^{\uparrow}$BW1; *b* – 6[4:14]6, specimen KMA-G5-140, LV, female, sample No. 14.2$^{\uparrow}$BW1; *c* – 5[4:14]5, specimen KMA-G5-114, RV, male, sample No. 14.2$^{\uparrow}$BW1; *d* – 6[11:0]6, specimen KMA-G5-114, RV, male, sample No. 14.2$^{\uparrow}$BW1; Kursk region, Mikhailovsky quarry section.

Fig. 5. Relationship between length (L) and height (H) of the shell in mm in studied specimens of Lophocythere tuberculata sp. nov. from the Early Callovian age, Mikhailovsky quarry section, boreholes No. 4 and No. 7 (Kursk region).

Fig. 6. Lophocythere mosaica sp. nov., SEM, *a* – *d* – external view, *a1* – *d1* – internal view: *a* – holotype KO2-161, Ad., RV, female, sample No. 4\116; *b* – specimen KO2-62, Ad., RV, female, sample No. 4\118; *c* – specimen KO2-101, Ad., LV, female, sample No. 4\118; *d* – specimen KO2-

96, A-2, sample No. 7\136. Kursk region: *a – c* – borehole No. 4; *d* – borehole No. 7; Lower Callovian, ammonite zones Gowerianus and Calloviense. Scale bar 100 μm.

Fig. 7. Evolution of representatives of the genus Lophocythere from the Callovian deposits of England, France and the European part of Russia, whose representatives are found in the Middle Russian Sea: *a* – the author's latest proposed reconstruction of relationships based on studied material (in the Bathonian age according to literature data – Malz, 1975: L. batei, p. 127, Table 1, fig. 6, RV, female; L. propinqua, p. 129, Table 4, fig. 29, LV, female; L. carinata, p. 132, Table 3, fig. 17, LV, female); *b* , *c* – views of different authors: *b* – Sheppard, 1981; *c* – Shurupova, Tesakova, 2019.

Explanation to Table VI

Left valves of Lophocythere shells, external view, SEM, scale bar 100 μm.

Fig. 1–3. Lophocythere interrupta Triebel, 1955: 1 – specimen KMA2-107, Ad., female; 2 – specimen Kursk-8, A-4; 3 – specimen KMA3-14, A-6; Lower Callovian, Mikhailovsky quarry section (Kursk region), all specimens from sample No. KMA-8.

Fig. 4-6. Lophocythere acrolophos Whatley, Ballent et Armitage, 2001: 4 - specimen MC2-115, Ad., female; 5 - specimen MC2-408, A-2; 6 - specimen MC2-403, A-4; Upper Callovian, Mikhailovcement section (Ryazan Region), all specimens from sample No. 13, Athleta ammonite zone.

Fig. 7-9. Lophocythere karpinskyi (Mandelstam in Lyubimova, 1955): 7 - specimen MC2-16, female; 8 - specimen MC2-20, A-3; 9 - specimen MC2-24, A-4; Upper Callovian, Mikhailovcement section (Ryazan Region), all specimens from sample No. 8, Coronatum ammonite zone.

Fig. 10-12. Lophocythere scabra Triebel, 1951: 10 - specimen KMA2-6, Ad., female, sample No. KMA-7; 11 - specimen KMA-41, sample No. KMA-7, A-2; 12 - specimen KMA-36, A-5, sample No. KMA-6; Lower Callovian, Mikhailovsky mine section (Kursk Region).

Fig. 13-15. Lophocythere bucki Lutze, 1960: 13 - specimen MC2-313, Ad., female, sample No. 15; 14 - specimen MC-342, A-3, sample No. 13; 15 - specimen MC2-351, A-4, sample No. 14; Upper Callovian, Mikhailovcement section (Ryazan Region), Athleta ammonite zone.

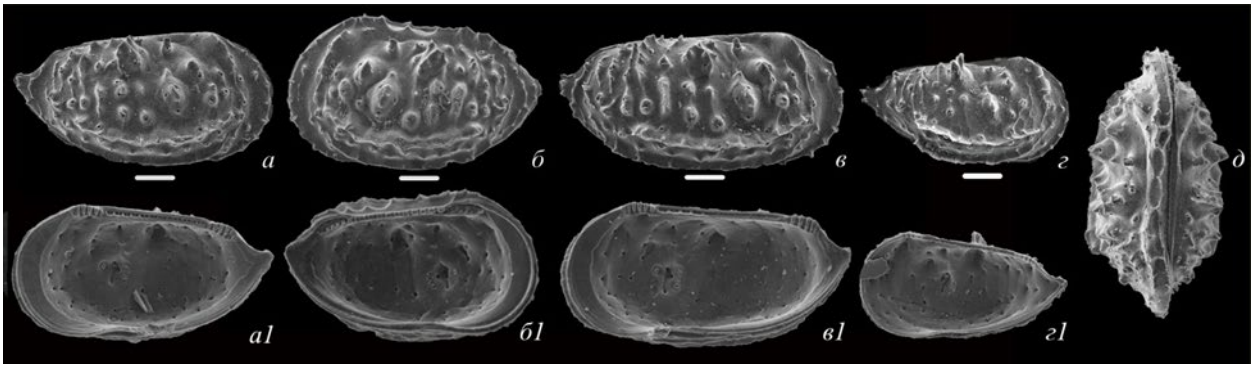

Fig. 1

Стадии онтогенеза	*L. tuberculata* sp. nov.
Adult	
A-1	
A-2	
A-3	
A-4	

Fig. 2

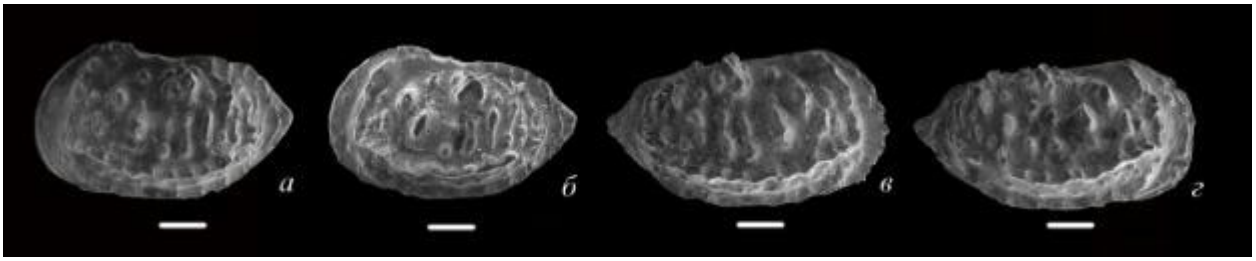

Fig. 3

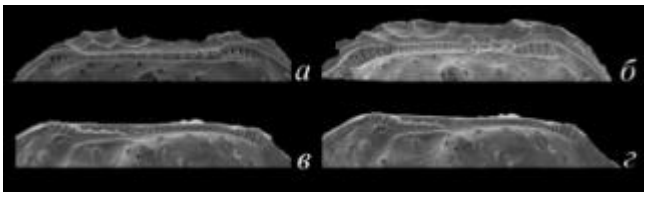
а
б
в
г

Fig. 4

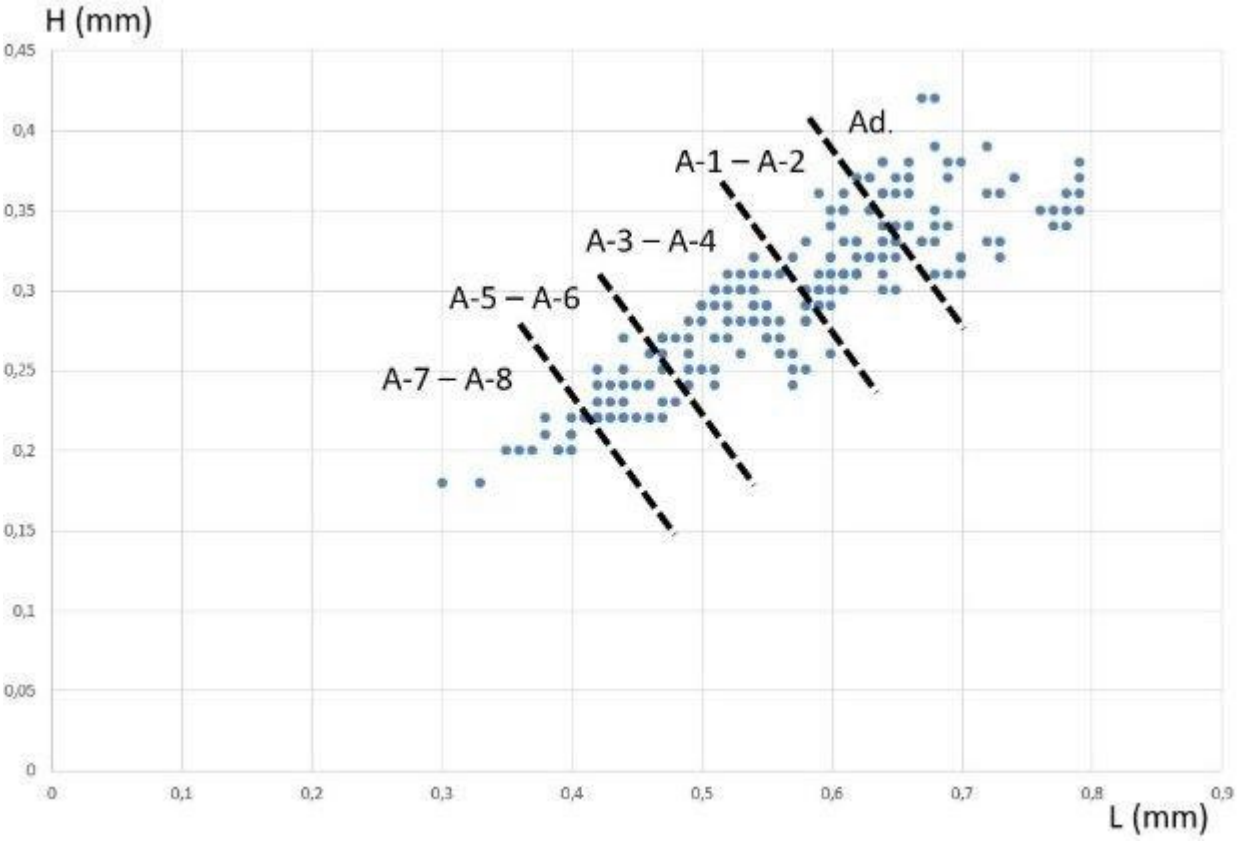
H (mm)
0,45
0,4
0,35
0,3
0,25
0,2
0,15
0,1
0,05
0
0
0,1
0,2
0,3
0,4
0,5
0,6
0,7
0,8
0,9
L (mm)
Ad.
A-1 – A-2
A-3 – A-4
A-5 – A-6
A-7 – A-8

Fig. 5

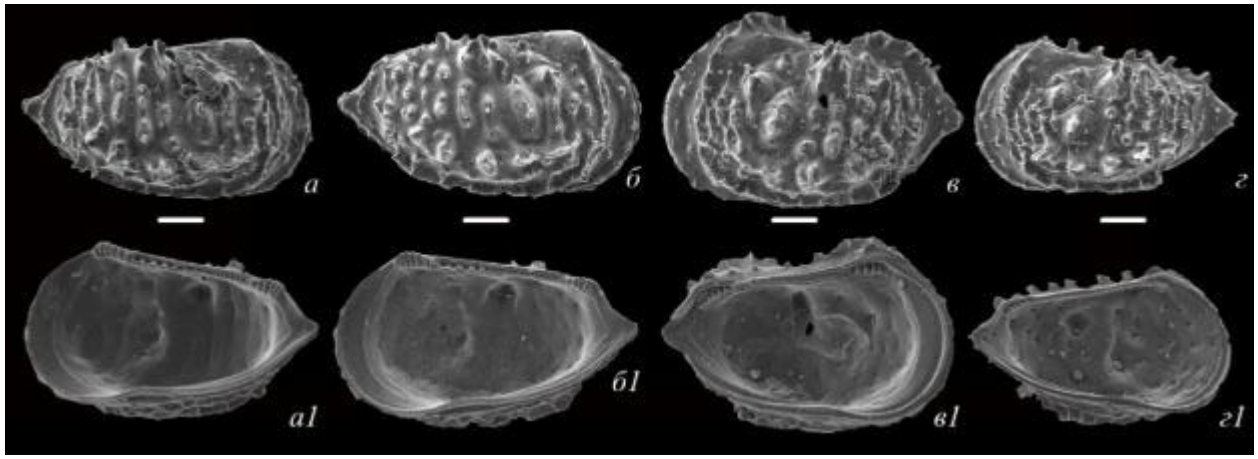
а
б
в
г
а1
б1
в1
г1

Fig. 6

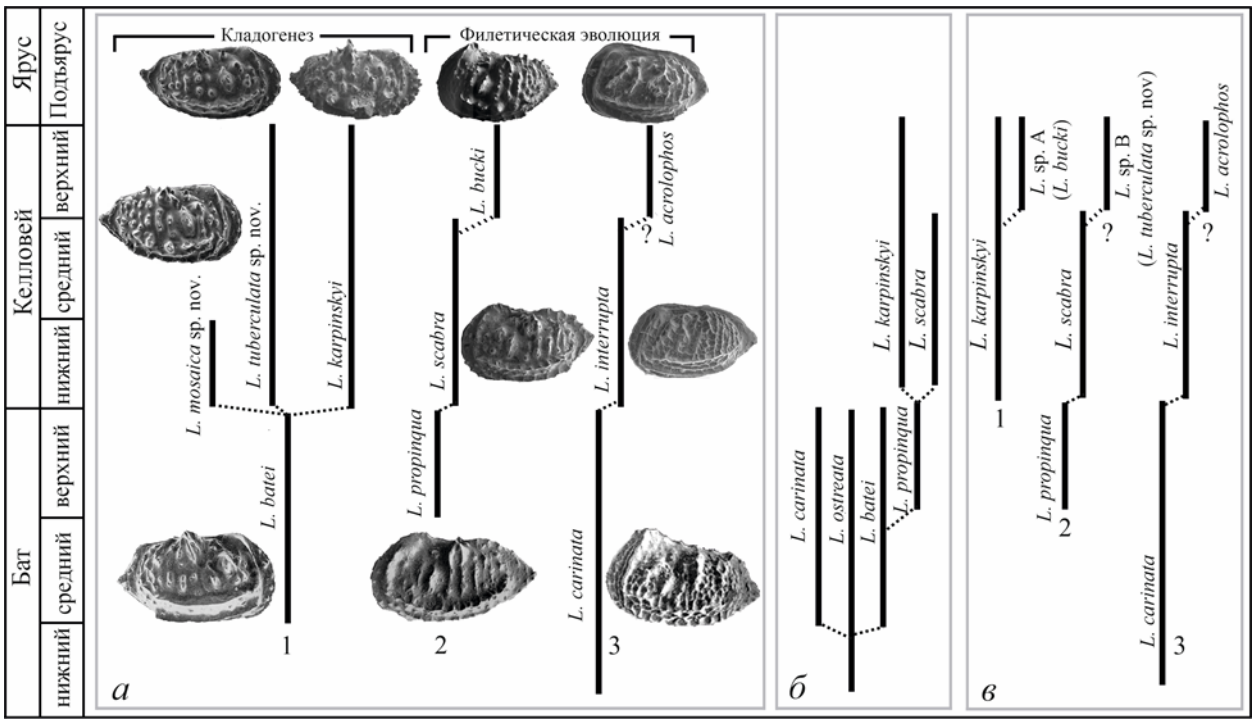
Ярус
Подъярус
Келловей
верхний
средний
нижний
Бат
верхний
средний
нижний
Кладогенез
Филетическая эволюция
L. mosaica sp. nov.
L. tuberculata sp. nov.
L. karpinskyi
L. batei
L. bucki
L. scabra
L. propinqua
L. interrupta
L. acrolophos
L. carinata
1
2
3
?
а
L. carinata
L. ostreata
L. batei
L. propinqua
L. scabra
L. karpinskyi
б
L. karpinskyi
L. sp. A
(L. bucki)
L. scabra
L. sp. B
(L. tuberculata sp. nov)
L. interrupta
L. acrolophos
L. propinqua
L. carinata
1
2
3
?
в

Fig. 7

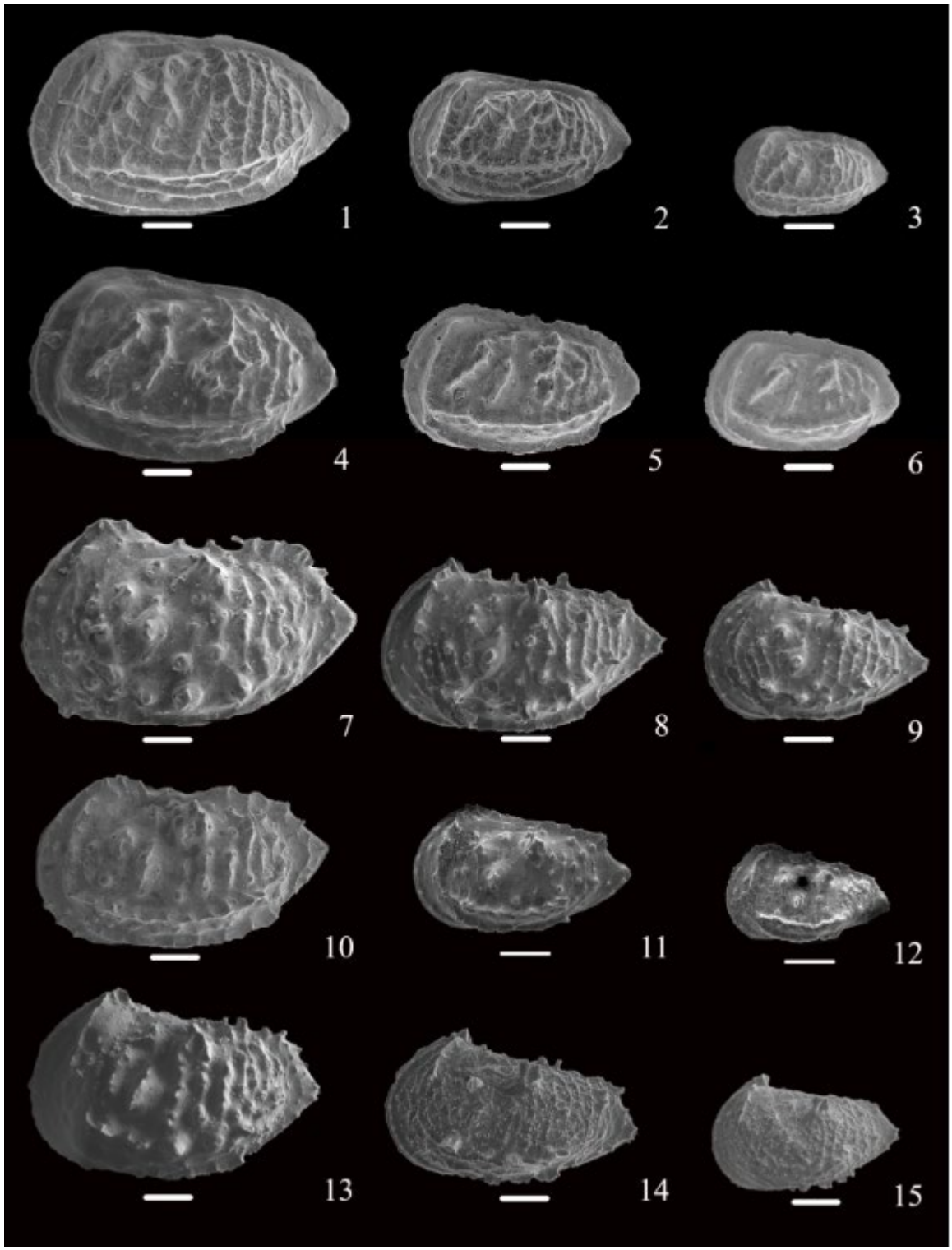
1
2
3
4
5
6
7
8
9
10
11
12
13
14
15